Tunable Stiffness Caudal Peduncle Leads to Higher Swimming Speed Without Extra Energy

Sijia Liu, Chunbao Liu, Yunhong Liang, Luquan Ren, and Lei Ren

***Abstract*—Tuning body stiffness like fish to improve swimming efficiency and speed has been adopted by many fish-inspired robotics. However, it is unknown whether the energy saved from improved efficiency can compensate for the energy consumption brought by tuning stiffness itself. To explore this issue, we develop a robotic fish with a tunable stiffness caudal peduncle (TSCP), simultaneously allowing for untethered swimming and online tunable stiffness, and conduct a series of tests. We first apply interchangeable caudal peduncles to our robot to explore the effect of a tunable stiffness mechanism and determine the optimal tunable stiffness interval. The results show that tunable stiffness can significantly improve the response of robot at different frequencies. Then we develop the TSCP by embedding shape memory alloy wire into a silicone matrix. TSCP can adjust the stiffness in real time through current and increase the initial stiffness by up to 57.4%. More importantly, we incorporate the cost of tunable stiffness into the total cost of transport compared to previous robots for the first time. The cost of maintaining medium and maximum stiffness accounts for 8.72% and 17.87% of the total cost of transport, respectively. As a result, TSCP increases the swimming speed by up to 35.5% and reduces the Strouhal number by up to 21.9% at high frequencies without extra power. This study supports the necessity of applying tunable stiffness to robotic fish and offers a novel idea for online tunable stiffness mechanism.**

***Index Terms*—Soft robotic fish, tunable stiffness caudal peduncle, shape memory alloy, untethered swimming.**

Manuscript received 17 April 2023; accepted 20 July 2023. Date of publication 1 August 2023; date of current version 9 August 2023. This letter was recommended for publication by Associate Editor P. Chirarattananon and Editor Y.-L. Park upon evaluation of the reviewers' comments. This work was supported in part by the Projects of National Natural Science Foundation of China under Grants 52075216, 91948302, and 91848204, in part by the Fundamental Research Funds for the Central Universities, Jilin University under Grant 2022-JCXK-15, and in part by Jilin Scientific and Technological Development Program under Grant 3D5224054428. *(Corresponding authors: Chunbao Liu; Lei Ren.)*

Sijia Liu is with the School of Mechanical and Aerospace Engineering, Jilin University, Changchun 130022, China (e-mail: liusj21@mails.jlu.edu.cn).

Chunbao Liu is with the School of Mechanical and Aerospace Engineering, Jilin University, Changchun 130022, China, and also with the Key Laboratory of CNC Equipment Reliability Ministry of Education, Jilin University, Changchun 130000, China (e-mail: liuchunbao@jlu.edu.cn).

Yunhong Liang and Luquan Ren are with the Key Laboratory of Bionic Engineering, Ministry of Education, Jilin University, Changchun 130022, China (e-mail: liangyunhong@jlu.edu.cn; lqren@jlu.edu.cn).

Lei Ren is with the Key Laboratory of Bionic Engineering, Ministry of Education, Jilin University, Changchun 130022, China, and also with the School of Mechanical, Aerospace and Civil Engineering, University of Manchester, M13 9PL Manchester, U.K. (e-mail: lei.ren@manchester.ac.uk).

This letter has supplementary downloadable material available at https://doi.org/10.1109/LRA.2023.3300587, provided by the authors.

Digital Object Identifier 10.1109/LRA.2023.3300587

I. Introduction

Apart from the unique propulsion mechanism, another key reason why fish maintain such high swimming efficiency is the flexibility of their bodies [1], [2]. Fish with flexible bodies enjoy many advantages, including low drag and energy consumption, high maneuverability, and environmental adaptability [3]. Stiffness is one of the important criteria for measuring flexibility. Due to the close interaction with the aquatic environment, the fish bodies have a range of possible functions beyond traditional forceful deformation and act more like a "hybrid oscillator" [4], [5]. This property is susceptible to stiffness [6]. To survive in the complex aquatic environment, fish have developed a critical ability: tunable stiffness [7].

It has been demonstrated in physiology that fish adjust their body stiffness through the antagonism of axial muscles [5], [8], [9]. This raises two questions. The first question is why adjust the stiffness. Quinn and Lauder proposed that there is no one "best" stiffness that always satisfies the demands [10]. The optimal stiffness tends to be different for different external inputs. Thus, the strategy of tunable stiffness is similar to car transmissions, aiming to strengthen speed or torque to match the environment. The second question is whether it is worth the costs. It is obvious that muscle antagonism means doing negative work, which requires extra energy. After simulating lampreys, Tytell et al. speculated that the negative work could strengthen the tail, and the energy saved from improved efficiency may compensate for the loss of negative work [11]. But this conclusion has yet to be widely supported by data.

Engineers have built many physical models to further study the tunable stiffness mechanism [6], [7], [12], [13], [14], [15], [16], [17], [18], [19], [20]. The most common approach is to adjust the body stiffness of a fixed mechanically-actuated passive flapping model by tension or antagonism, and measure the thrust in a recirculating flow tank. Most such stiffness optimization methods allow robots to continuously tune stiffness while swimming [10], which can be summarized as online tunable stiffness. For example, Zhong et al. reported that to maximize efficiency, muscle tension should scale with swimming speed squared, and tunable stiffness could double swimming efficiency at tuna-like frequencies and speeds (Table I a) [20]. Park et al. presented a novel variable-stiffness flapping (VaSF) mechanism that could change its stiffness to maximize the thrust of a bio-inspired underwater robot (Table I b) [21]. Wolf et al. used a pneumatically-actuated fish-like model to investigate how antagonistic drive affected locomotor force generation, and

TABLE I
CHARACTERISTIC PARAMETERS OF THE SILICONE [14], [20], [22], [24], [26], [30], [31]

Item	Schemata	Mechanism
a	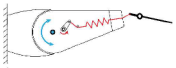	Tensional spring
b		Tensional cable
c		Antagonistic air pressure
d		Replaceable spring plate
e	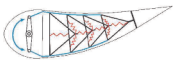	Antagonistic tensegrity
f		Replaceable torsion spring
g		tunable torque motor

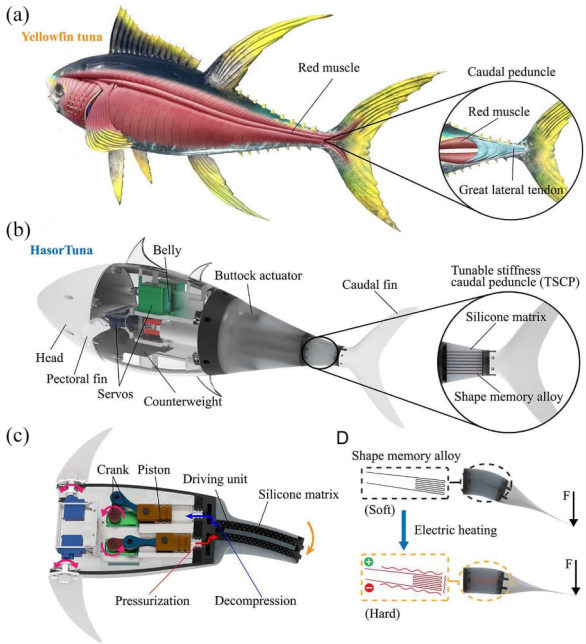

Fig. 1. Overview design of the robotic fish. (a) Muscle system and caudal peduncle structure of the bionic prototype-yellowfin tuna, (b) overview and caudal peduncle structure of HasorTuna, (c) schematic diagram and mechanism of the pectoral fins and hydraulic system and (d) schematic diagram of the tunable stiffness mechanism.

reported that stiffness and frequency had complex interactive effects on thrust (Table I c) [14]. However, the robots in these examples were all fixed in holders and swam tethered, which could not obtain the swimming speed accurately.

Untethered fish-inspired robots are also essential platforms for testing biological hypotheses [10]. Tunable stiffness has become one of the mainstream methods to enhance the performance of existing robots [22], [23]. The most common solution is to apply elastic parts of different stiffness to robots. For example, there have been passive interchangeable caudal peduncles made with elastic sheets or torsion springs [1], [2], [24], [25], [26], [27]. Other methods of tunable stiffness include applying nylon inserts [28], extra vertebrae [29] and tensegrity structures [22], [30]. Several typical robots are listed in Table I d, e and f. The stiffness optimization methods described above can be summarized as offline, that is, tunable stiffness requires stopping swimming and manual intervention, in which the energy cost of converting stiffness cannot be measured. Yu et al. reported a robotic dolphin that could adjust the passive torque of the caudal peduncle motor, allowing for both untethered swimming and online tunable stiffness, as listed in Table I g [24]. However, they focused on the leaping ability of the robot rather than the cost of transport.

The primary objective of this study is to find out whether the tunable stiffness increases the cost of transport. To this end, we developed a soft robotic fish that integrated both the online tunable stiffness and untethered swimming ability. The robot was equipped with a new tunable stiffness caudal peduncle (TSCP) with shape memory alloy (SMA). In swimming, the SMA wire is heated and hardened to alter the stiffness of caudal peduncle. This adjustment mechanism theoretically has an infinite number of stiffnesses, and allows the robot to modulate the power transmitted from body to caudal fin. Moreover, we conducted a series of tunable stiffness swimming experiments. The results showed that the designed tunable stiffness mechanism could significantly optimize the propulsion speed and efficiency. In particular, we found that at higher frequencies, the energy saved by tuning stiffness could compensate for the energy consumption brought by tuning stiffness itself. This finding may explain the important biological hypothesis: the energetic benefits of altering stiffness may be worth the costs.

II. METHODS

A. Overview of the Robotic Fish

We developed a Hydraulic Autonomous Soft Robotic Tuna (HasorTuna) to achieve high frequency and efficient swimming. As illustrated in Fig. 1(a) and (b), the body profile of HasorTuna is designed based on the appearance of yellowfin tuna. The structure of HasorTuna can be divided into five sections: head, belly, buttock, caudal peduncle and caudal fin. The head is equipped with a control system, including microcontroller unit (MCU), Bluetooth chip, power sensor, battery, and transformer. A pair of pectoral fins and a hydraulic pump are integrated into the belly.

As shown in Fig. 1(c), the pectoral fins are individually driven by two servos and allow HasorTuna to submergence-emergence by changing the angle of attack. The hydraulic pump and buttock soft actuator form a complete hydraulic driving system. The servos actuate pistons to pump hydraulic oil into the driving units by a crank–slider mechanism. The soft actuator consists of driving units and a silicone matrix. McKibben artificial muscles as driving units expand radially and contract axially under pressure, like biological muscles [32]. The driving units are arranged parallelly on both sides of the body axis, mimicking the red

TABLE II
TECHNICAL SPECIFICATIONS OF HASORTUNA

Item	Specifications
Dimensions	576 mm (L) × 220 mm (W) × 180 mm (H)
Weight	3.5 kg
MCU	Arduino Nano RP2040 Connect
Servos	15 kg.cm × 2 (pectoral fin) 60 kg.cm × 2 (buttock actuator)
Power sensor	MAX471
Pressure sensor	XGZP6869A
Communication	Bluetooth/HC-06
Battery	Li-ion 12V 1500 mAh × 2

TABLE III
CHARACTERISTIC PARAMETERS OF THE SILICONE

Item	Tensile Strength	100% Modulus	Shore Hardness
EC50	315 psi	12 psi	00-50
DR10	475 psi	22 psi	10A
DR20	550 psi	49 psi	20A
EC30	200 psi	10 psi	00-30

muscles, as shown in Fig. 1(a) [33]. The silicone matrix fixes and protects the driving units, mimicking the connective tissue. The materials of the silicone matrix and the inner hose inside the driving units are Ecoflex 00-50 (EC50) and Dragon Skin 10 (DR10) silicone, respectively. Table III shows the characteristic parameters of the silicone. The differential rotation of the servos provides pressure pulses for the soft actuator. When pressing hydraulic oil into one side driving units to deflect the matrix, the hydraulic pump sucks out hydraulic oil from the other side driving units. The rotational velocity and angle of the servos control the tail-beat frequency and amplitude.

The peripheral components of HasorTuna were 3D printed, including the pectoral and caudal fins. The main components of the hydraulic pump were machined from aluminum alloy. We placed a pair of lead blocks below the buoyancy center to regulate the barycenter and prevent lateral roll. The main specifications are presented in Table II.

B. Tunable Stiffness Mechanism

Two issues must be considered before designing the tunable stiffness mechanism: where and how. As a rule, fish adjust their stiffness across the entire body. However, the caudal peduncle at the base of the tail is considered the key region for stiffness modulation [19]. This region acts more as a passive joint, adjusting the force transmitted from the body to the tail by varying stiffness, although it can actively bend. The tendons of caudal peduncle extend to the tail, as shown in Fig. 1(a). The body muscles stiffen the tendons through antagonistic movements, thus strengthening the caudal peduncle [34]. Moreover, many studies have taken the caudal peduncle as a part of their robotic fish design [1], [3], [20], [24], [25], [26], [27], [31], [35]. Therefore, we set the tunable stiffness mechanism at the caudal peduncle.

The second issue is how to achieve the tunable stiffness. An intuitive method is to replace the torsion springs or elastic sheets with different stiffnesses. But this method is offline and cannot be measured for the energy cost of tuning stiffness. Many researchers achieved online tunable stiffness

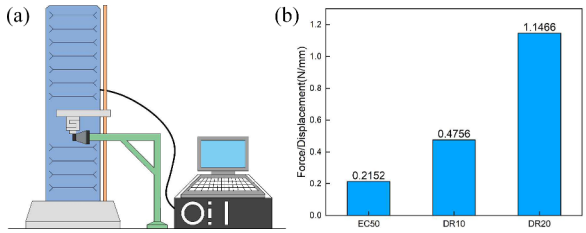

Fig. 2. Stiffness test of the caudal peduncles: (a) test diagram, (b) test results.

models with antagonistically-control, mechanically-control or structurally-control, which need additional motors or complex components. [10]. However, they are not suitable for untethered robots with strict requirements on sealing, mass distribution and volume. Theoretically, the stiffness of robots can be tuned by altering the intrinsic material properties of its elastic elements. Smart-material-based stiffness adjustment techniques make this strategy feasible, especially for soft continuum robots. Various studies demonstrated that variable stiffness structures using embedded thermal phase transition materials could undergo a significant stiffness variation by heating. This concept can be easily integrated with other types of structures with compact configurations [36]. In this study, we used a SMA (Ni-Ti alloy) wire folded into a serpentine shape as insert material to tune stiffness and a silicone matrix as outer material to shape and seal the TSCP, as shown in Fig. 1(b). During the transformation from the martensitic phase to the austenitic phase after heating, SMA can not only "remember shape", but also increase its elastic modulus, as illustrated in Fig. 1(d). More importantly, SMA remains in the same energy flow direction as fish, i.e., consuming energy to stiffen, even if their mechanisms are different. As a result, we can regulate the heating temperature on SMA by altering the current and thus continuously tune the stiffness of TSCP.

III. RESULTS

A. Offline Tunable Stiffness

The caudal peduncle can modulate the power transmitted to the caudal fin, and the effect is generally governed by stiffness. To explore the effect of a tunable stiffness mechanism and determine the optimal range of tunable stiffness, we first fabricated three caudal peduncles with different materials to achieve a large range of stiffness variation. The caudal peduncles are made of EC50, DR10 and Dragon Skin 20 (DR20) silicone, respectively. Table III shows the characteristic parameters of the silicone. We tested the bending stiffness of the three caudal peduncles on a tensile machine, as shown in Fig. 2(a). The end of the caudal peduncle close to the body was fixed to a bracket. The tensile machine applied pressure to the free end to twist the caudal peduncle and continuously recorded the force (F) and displacement (D) of the indenter. The stiffness of the caudal peduncle is given by

$$\text{Stiffness} = \frac{F}{D}, \tag{1}$$

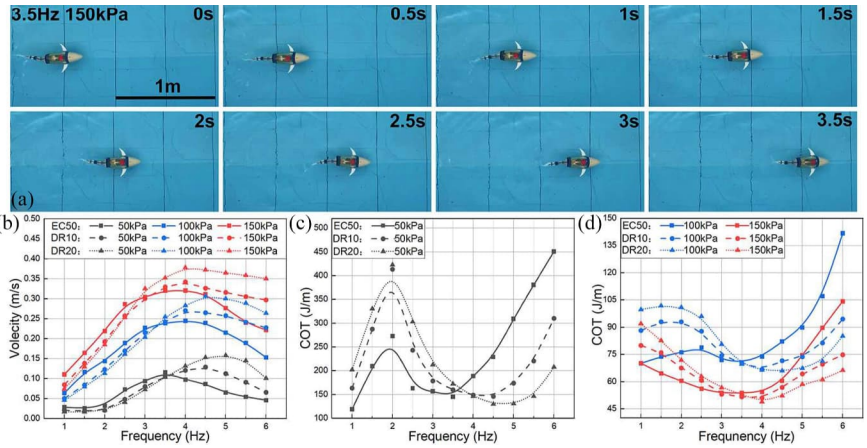

Fig. 3. Swimming performance of HasorTuna with three caudal peduncles: (a) Snapshots of swimming at 3.5 Hz and 150 kPa, (b) swimming speed, (c) COT for 50 kPa, (d) COT for 100, and 150 kPa.

The relationship between F and D was linear and we found the slope as stiffness. The stiffness of the three caudal peduncles is shown in Fig. 2(b).

We used a CPG control model based on Hopf oscillator to control the oil pressure. To reduce the pressure control error, a proportional"integral"derivative (PID) controller was added to form a closed-loop control system. Two miniature pressure sensors connected to the hydraulic flow path measured the hydraulic pressure of the driving units on both sides, respectively. The MCU converted the analog signals of the pressure sensors into a digital signal through Digital to Analog Converter (ADC) and made them as the feedback of the PID controller. HasorTuna connected to a laptop through Bluetooth to obtain control parameters such as frequency and pressure. The free swimming was conducted in a water tank with a size of 4 m $\times$ 2 m $\times$ 1 m. A red sticker was attached to the dorsal fin of HasorTuna to mark the location in the experiments. A global vision camera (FUJIFILM XT30 II, 1920 $\times$ 1080, 60 fps) was placed above the tank to record the swimming process. The robot maintained straight swimming throughout the test. For better stability and wireless signal transmission while swimming, HasorTuna maintained slightly positive buoyancy. Fig. 3(a) shows the snapshots of straight swimming at a driving pressure of 150 kPa and a driving frequency of 3.5 Hz. In the test, the steady speed is determined by calculating the average swimming speed over the last half interval.

Fig. 3(b) shows the swimming speed of HasorTuna at frequencies of 1–6 Hz and pressures of 50, 100 and 150 kPa. Undoubtedly, the higher pressure led to greater oscillations, and thus increased speed. Fish-inspired robots are sensitive to frequency, especially the ones with flexible passive components. Experimental results showed that the relationship between speed and frequency was not linear. At the same pressure, regardless of the caudal peduncle stiffness, the swimming speed first increased and then decreased with frequency. A stiffer caudal peduncle led to the inflection points of the trend shifting toward higher frequencies. Meanwhile, with the same input conditions, the softer caudal peduncle performed better at low frequencies, while the stiffer one was suitable for high frequencies. A similar situation occurred in the cost of transport (COT) of HasorTuna. COT is the energy consumption per unit distance, and is defined as:

$$COT = \frac{Q}{l} = \frac{P_t}{U}, \tag{2}$$

where Q is the energy consumption, l is the swimming distance and P_t is the total power. COT is an indicator that directly reflects the range and efficiency of robots. In this study, we considered the power of the driving system as the total power and ignore the small power of MCU and Bluetooth. A power detection chip (MAX451) continuously monitored the voltage and current of servos. We computed the average power by integrating the instantaneous power. Fig. 3(c) and (d) show the COT of HasorTuna. It is obvious that the COT is negatively correlated with the driving pressure. The COT curves are roughly U-shaped, with the inflection points approximately corresponding to the maximum swimming speed. Notice that there are clear spikes in the COT near 2 Hz at 50 kPa. This is because too small a tail-beat amplitude cannot generate enough thrust at low frequencies. The speed remained constant as the frequency increased, leading to an increase in COT. The situation was improved as the driving pressure increased. At low frequencies, the softer caudal peduncle corresponded to a smaller COT, and the situation was reversed at high frequencies.

According to the experimental results, the stiffness of the caudal peduncle significantly affected the swimming performance. The extreme points of the COT and speed shifted to higher frequencies as the caudal peduncle stiffness increased, indicating that the stiffer caudal peduncle adapted to higher frequency intervals. In particular, the softer caudal peduncle was better than the stiffer one at lower frequencies, while the stiffer one gradually showed more advantages as the frequency increased. In Fig. 4, we plotted the midline displacements of HasorTuna during a single tail-beat cycle at 150 kPa to explore how caudal peduncle stiffness influenced swimming performance. For fish, one of the secrets to maintain high swimming efficiency is to

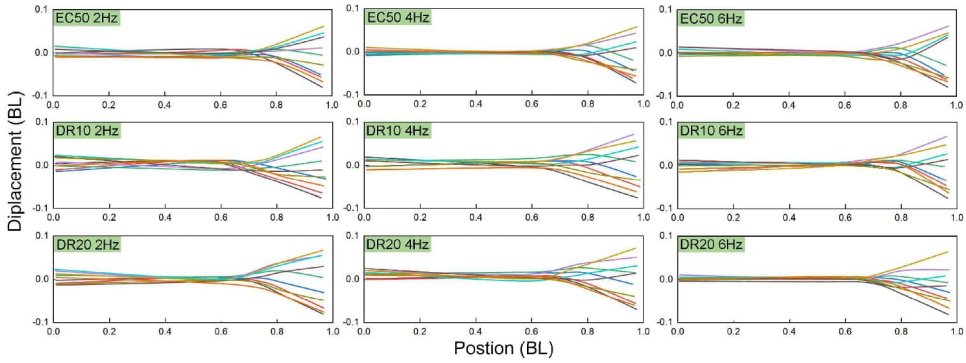

Fig. 4. Midline displacements of HasorTuna at equal time intervals during a single tail-beat cycle.

control the angle of attack of caudal fin. Too small angle of attack cannot produce enough thrust, while too much will cause dynamic stall and reduce thrust [37]. Only the proper angle of attack can produce thrust efficiently. For example, fish always maintain their tail angle of attack around 20° [35]. At low frequencies, the small lateral swing speed of the caudal fin leads to little lateral force. The softer caudal peduncle can increase the angle of attack to a good range under little lateral force. As the frequency increases, higher lateral force would result in excessive angle of attack and even dynamic stall, which reduces the thrust. Therefore, properly strengthening the caudal peduncle can effectively suppress the angle of attack in a good range at high frequencies. The midline displacements in Fig. 4 reflect the regulating effect of the different stiffness caudal peduncle on angle of attack. At low frequencies, the softer caudal peduncle had a larger angle of attack and led to faster swimming. As the frequency increased, the stiffer caudal peduncle effectively suppressed the excessive angle of attack. Therefore, there is no doubt that tunable stiffness has a positive effect on the hydrodynamic characteristics of the tail, increasing thrust and efficiency.

B. Online Tunable Stiffness

Tuning stiffness while swimming, i.e., online, is essential for roboticists who want their robots to adapt to changing conditions. For our robot, we can regulate the temperature of the SMA to achieve online tunable stiffness. The MCU controls the current through the SMA with Pulse Width Modulation (PWM) signal to regulate the caudal peduncle stiffness, as shown in Fig. 5(a). The stiffness variation of SMA is limited, so we need to find an appropriate stiffness variation range for TSCP. From EC50 to DR10, HasorTuna achieved larger spans in speed and COT with a smaller change in stiffness. Therefore, we set the stiffness range of TSCP between EC50 and DR10. We chose Ecoflex 00-30 (EC30) silicone, which was slightly softer than EC50, as the external matrix material for TSCP to ensure that its stiffness was within the selected range after embedding SMA. The characteristic parameters of EC30 are shown in Table II. The inner SMA wire is folded into a serpentine shape to increase its original stiffness by a factor of seven. We measured the underwater stiffness of TSCP and temperature of the inner SMA

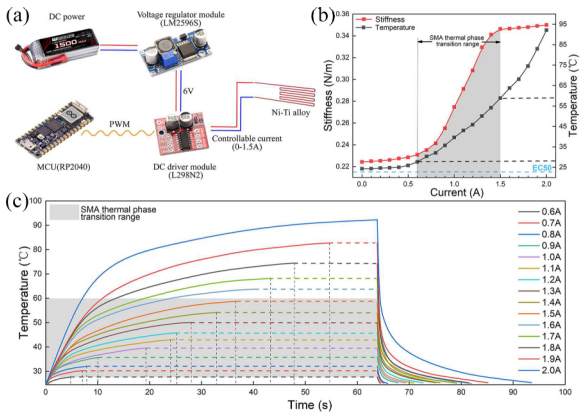

Fig. 5. (a) Control circuit of TSCP, (b) caudal peduncle stiffness and SMA temperature at different currents, and (c) SMA temperature response.

with the tensile machine and a thermocouple sensor (TCM-UA), respectively. The results are illustrated in Fig. 5(b). The SMA has a thermal phase transition range of approximately 27–58 °C, corresponding to a current of 0.6–1.5 A. The stiffness of TSCP with 0 A and 2 A is 0.2242 and 0.3528 N/mm, respectively, which means that TSCP can increase the initial stiffness by up to 57.4% through the thermal phase transition. We set the current at 0, 1, and 1.5 A in the test to cover the stiffness interval, and the stiffness of 1 A and 1.5 A was 0.2747 and 0.3463 N/mm, respectively.

We recorded the temperature response of underwater TSCP at a rate of 10 Hz, as shown in Fig. 5(c). The time for TSCP to reach the stable temperature was 19.4 s and 35.6 s under the constant current of 1.0 A and 1.5 A, respectively. The temperature dropped below the initial phase transition temperature within 10 s. In the swimming test, the SMA was powered up for 40 s to ensure that the stiffness transition was complete before swimming. The current remained constant in single swimming. The steady speeds of TSCP at different currents are presented in Fig. 6(a), (b) and (c). TSCP had the same speed tendency as above replaceable caudal peduncles: the speeds of smaller stiffness were faster at low frequencies, while the larger stiffness was more advantageous with increasing frequencies. This property is independent of the driving pressure.

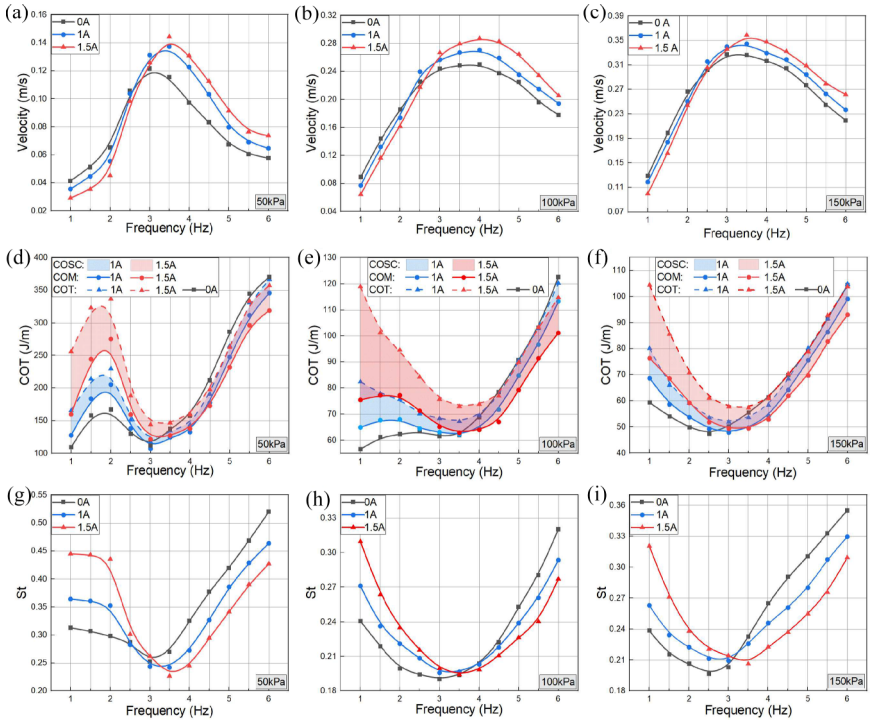

Fig. 6. Performance of HasorTuna with TSCP under 50, 100, and 150 kPa: (a–c) swimming speed, (d–f) COT, (g–i) St.

To more accurately reflect the COT of HasorTuna, we monitored the power consumed by TSCP with an additional MAX451. In the experiments, the power of TSCP was the cost of stiffness change ($COSC$) with power of 1.35 w and 2.80 w at 1 A and 1.5 A, respectively. The other MAX451 monitored the cost of motors (COM). Thus, the total COT of HasorTuna is the sum of $COSC$ and COM. Specifically, COM is equal to COT as $COSC$ is zero at 0 A. Fig. 6(d), (e) and (f) plot the detailed power consumption of HasorTuna. TSCP had a COM similar to the COT of the interchangeable caudal peduncles above: smaller stiffness consumed less energy at low frequencies, while larger stiffness was more advantageous as frequency increased. The COT of softer TSCP was significantly lower at low frequencies. The COT of 1 A started to approach or even fall below that of 0 A at the frequencies corresponding to the peak speeds, and each stiffness had close COT as the frequency continued to increase, while the speeds of stiffer TSCP were faster. This indicated that TSCP could improve the speed by adjusting its stiffness in a specific frequency range without extra energy. As shown in Fig. 6(a), (d), TSCP with 1.5 A could increase the speed of 0 A by up to 35.5% without increasing COT at 50 kPa, 5 Hz. At this point the speeds of 0 A and 1.5 A were 0.06749 and 0.09148 m/s, respectively.

The Strouhal number (St) is an important dimensionless parameter for describing the tail or wing kinematics of swimming and flying animals [38]. It is known to govern a well-defined series of vortex growth and shedding regimes for airfoils undergoing pitching and heaving motions [39]. St is defined as

$$St = \frac{fA}{U}, \tag{3}$$

where f is the tail-beat frequency, A is the peak-to-peak amplitude of the tail-beat, and U is the forward speed. St is inversely proportional to efficiency [40]. Usually, most aquatic animals, like dolphins, sharks and bony fish, have a narrow range (0.2–0.4) of St for maximizing propulsive efficiency [41]. Fig. 6(g), (h), and (i) plot St of HasorTuna in different states. The main distribution of St for 50 kPa was in the range of 0.22–0.53, which exceeded the optimal range. Increasing the driving pressure to 100 kPa and 150 kPa could reduce St into the optimal range. Similar to the speed and COT, the minimum values of St moved towards the higher frequencies with increasing stiffness. Furthermore, the lower St of stiffer TSCP demonstrated that tunable stiffness could increase propulsion efficiency obviously. Results showed that TSCP with 1.5 A could reduce the St of 0 A by up to 21.9% without extra COT at 50 kPa, 4.5 Hz, and the St of 1.5 A and 0 A is 0.29493 and 0.37772, respectively.

C. Swimming Pool Test

In order to further verify the practicability of TSCP, we conducted a long-distance test in a 50 m long swimming pool, as shown in Fig. 7(a) and (b). The goal of the test to compare the difference between no stiffness adjustment and optimal stiffness adjustment based on TSCP for the given continuous frequencies 3, 4 and 5 Hz and 150 kPa. HasorTuna swam 3 × 50 m with an optimal tuning stiffness strategy (3 Hz-0 A, 4 Hz-1 A, and 5 Hz-1.5 A), respectively. The control group completed the test with the fixed stiffness of 0 A. The experimental results are illustrated in Fig. 7(c). For the same swimming distance of 150 m, the fixed stiffness caudal peduncle and TSCP had

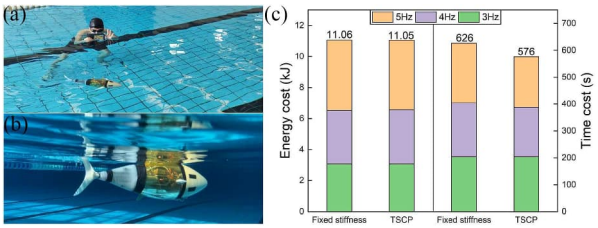

Fig. 7. (a, b) Test in swimming pool, (c) energy and time cost of Fixed stiffness caudal peduncle, and TSCP.

almost equal energy cost, but TSCP could save 8% time cost after stiffness modulation.

IV. Discussion

Body stiffness is an important feature for fish, which has increasingly been included in the design of aquatic robots [42], [43] and the computational analyses of fish-inspired movement [44], [45]. As the primary part connecting the body and tail, the tunable stiffness caudal peduncle has a positive regulating effect on swimming. In this study, we first applied the interchangeable caudal peduncles to our robot and demonstrated that tunable stiffness could indeed improve the performance of HasorTuna. The results showed that a more flexible caudal peduncle led to higher speeds at low frequencies, but the trend was reversed as the frequency increased. This feature is consistent with the physiological habits of fish. At low speeds, fish reduce the tail-beat frequency and relax their bodies to conserve energy. When feeding or escaping, the fish muscles produce antagonistic activity to increase body stiffness and generate higher speed or acceleration [46]. For example, the antagonistic electromyographic signal of Polypterus were recorded during some rapid C-start escape responses [47]. In addition, the test results helped us to find the appropriate tunable stiffness interval. We then developed TSCP based on the thermal phase transition mechanism of SMA. Control of the current flowing through the SMA enables continuous tuning of the caudal peduncle stiffness. TSCP has been proven effective in optimizing the hydrodynamic characteristics of the robot.

Until now, although there are many forms of tunable stiffness, untethered and online tunable stiffness seem irreconcilable for robotic fish. Our robot is one of the few robots that can coordinate the untethered swimming and online tunable stiffness at the same time, which can help us calculate the energy cost of tunable stiffness and add it to the total COT. In this study, we measured the COT of HasorTuna, including the energy consumption of the motors and the TSCP, respectively. Both TSCP and fish consume energy to increase their stiffness, although by different mechanisms. The experimental results of TSCP revealed an interesting fact: altering stiffness is worth the costs. Increasing stiffness means doing 'negative work', as in the antagonistic action of fish muscles. Negative work required extra energy, but the total COT did not increase and is even slightly lower at high frequencies, while corresponding to greater speed and efficiency. The efficiency enhanced from the tunable stiffness had been confirmed in St. The energy saved from tunable stiffness was enough to compensate for the TSCP consumption. It means that we can indeed improve the performance of robots with some active mechanisms without compromising the existing endurance mileage.

V. Conclusion and Future Work

The main objective of this study is to demonstrate the feasibility and necessity of adding an online tunable stiffness mechanism to a robot. We first fabricated interchangeable caudal peduncles in three different harnesses silicone and tested them on our robot. Results showed that interchangeable caudal peduncles could greatly improve swimming performance. Then we developed a novel tunable stiffness caudal peduncle (TSCP) based on the shape memory alloy wire, allowing continuous stiffness adjustment without pausing swimming. TSCP could increase the initial stiffness by up to 57.4%. In the tests, our robots could increase the swimming speed and efficiency without extra power. The results show that TSCP increased the speed by up to 35.5% and reduced St by up to 21.9% without extra energy at high frequencies. In brief, this study provides an innovative idea for improving the swimming performance of robotic fish and helps us to further understand the biomechanics in fish.

In future work, we will further extend the tunable stiffness range of TSCP and reduce its foundation stiffness to cover more frequency ranges. Also, online control based on intelligent algorithms will be considered to achieve adaptive swimming.

References

[1] Q. Zou, B. Lu, Y. Fu, X. Liao, Z. Zhang, and C. Zhou, "Dynamic modeling and optimization of robotic fish based on passive flexible mechanism," in *Proc. IEEE Int. Conf. Mechatron. Automat.*, 2021, pp. 622–627.

[2] D. Chen, Z. Wu, H. Dong, M. Tan, and J. Yu, "Exploration of swimming performance for a biomimetic multi-joint robotic fish with a compliant passive joint," *Bioinspiration Biomimetics*, vol. 16, no. 2, Dec. 2020, Art. no. 026007, doi: 10.1088/1748-3190/abc494.

[3] C. H. White, G. V. Lauder, and H. Bart-Smith, "Tunabot Flex: A tuna-inspired robot with body flexibility improves high-performance swimming," *Bioinspiration Biomimetics*, vol. 16, no. 2, Mar. 2021, Art. no. 026019, doi: 10.1088/1748-3190/abb86d.

[4] A. R. Blight, "The muscular control of vertebrate swimming movements," *Biol. Rev.*, vol. 52, no. 2, pp. 181–218, 1977, doi: 10.1111/j.1469-185X.1977.tb01349.x.

[5] J. long, H. John, and K. S. Nipper, "The importance of body stiffness in undulatory Propulsion1," *Amer. Zoologist*, vol. 36, no. 6, pp. 678–694, 2015, doi: 10.1093/icb/36.6.678.

[6] K. L. Feilich and G. V. Lauder, "Passive mechanical models of fish caudal fins: Effects of shape and stiffness on self-propulsion," *Bioinspiration Biomimetics*, vol. 10, no. 3, Apr. 2015, Art. no. 036002, doi: 10.1088/1748-3190/10/3/036002.

[7] Y. Luo, Q. Xiao, G. Shi, G. Pan, and D. Chen, "The effect of variable stiffness of tuna-like fish body and fin on swimming performance," *Bioinspiration Biomimetics*, vol. 16, no. 1, Nov. 2020, Art. no. 016003, doi: 10.1088/1748-3190/abb3b6.

[8] J. LONG and H. JOHN, "Muscles Elastic energy, and the dynamics of body stiffness in swimming Eels1," *Amer. Zoologist*, vol. 38, no. 4, pp. 771–792, 2015, doi: 10.1093/icb/38.4.771.

[9] J. Long, H. John, M. J. McHenry, and N. C. Boetticher, "Undulatory swimming: How traveling waves are produced and modulated in sunfish (Lepomis Gibbosus)," *J. Exp. Biol.*, vol. 192, no. 1, pp. 129–145, 1994, doi: 10.1242/jeb.192.1.129.

[10] D. Quinn and G. Lauder, "Tunable stiffness in fish robotics: Mechanisms and advantages," *Bioinspiration Biomimetics*, vol. 17, no. 1, Dec. 2021, Art. no. 011002, doi: 10.1088/1748-3190/ac3ca5.

[11] E. D. Tytell, C.-Y. Hsu, T. L. Williams, A. H. Cohen, and L. J. Fauci, "Interactions between internal forces, body stiffness, and fluid environment

in a neuromechanical model of lamprey swimming," *Proc. Nat. Acad. Sci.*, vol. 107, no. 46, pp. 19832–19837, 2010, doi: 10.1073/pnas.1011564107.
[12] Y. Zhang, R. Kang, D. Romano, P. Dario, and Z. Song, "Experimental research on the coupling relationship between fishtail stiffness and undulatory frequency," *Machines*, vol. 10, no. 3, 2022, Art. no. 182. [Online]. Available: https://www.mdpi.com/2075-1702/10/3/182
[13] R. M. Shelton, P. J. M. Thornycroft, and G. V. Lauder, "Undulatory locomotion of flexible foils as biomimetic models for understanding fish propulsion," *J. Exp. Biol.*, vol. 217, no. 12, pp. 2110–2120, 2014, doi: 10.1242/jeb.098046.
[14] Z. Wolf, A. Jusufi, D. M. Vogt, and G. V. Lauder, "Fish-like aquatic propulsion studied using a pneumatically-actuated soft-robotic model," *Bioinspiration Biomimetics*, vol. 15, no. 4, Jun. 2020, Art. no. 046008, doi: 10.1088/1748-3190/ab8d0f.
[15] Z. Cui and H. Jiang, "Modeling and analysis of a swimming tincaeus with bio-inspired stiffness profile," in *Proc. IEEE Int. Conf. Robot. Biomimetics*, 2015, pp. 273–278.
[16] A. K. Kancharala and M. K. Philen, "Optimal chordwise stiffness profiles of self-propelled flapping fins," *Bioinspiration Biomimetics*, vol. 11, no. 5, Sep. 2016, Art. no. 056016, doi: 10.1088/1748-3190/11/5/056016.
[17] A. Jusufi, D. M. Vogt, R. J. Wood, and G. V. Lauder, "Undulatory swimming performance and body stiffness modulation in a soft robotic fish-inspired physical model," *Soft Robot.*, vol. 4, no. 3, pp. 202–210, 2017, doi: 10.1089/soro.2016.0053.
[18] M. J. Mchenry, C. A. Pell, J. Long, and H. John, "Mechanical control of swimming speed: Stiffness and axial wave form in undulating fish models," *J. Exp. Biol.*, vol. 198, no. 11, pp. 2293–2305, 1995, doi: 10.1242/jeb.198.11.2293.
[19] D. G. Matthews, R. Zhu, J. Wang, H. Dong, H. Bart-Smith, and G. Lauder, "Role of the caudal peduncle in a fish-inspired robotic model: How changing stiffness and angle of attack affects swimming performance," *Bioinspiration Biomimetics*, vol. 17, no. 6, Oct. 2022, Art. no. 066017, doi: 10.1088/1748-3190/ac9879.
[20] Q. Zhong et al., "Tunable stiffness enables fast and efficient swimming in fish-like robots," *Sci. Robot.*, vol. 6, no. 57, Art. no. eabe4088, 2021, doi: 10.1126/scirobotics.abe4088.
[21] Y.-J. Park, T. M. Huh, D. Park, and K.-J. Cho, "Design of a variable-stiffness flapping mechanism for maximizing the thrust of a bio-inspired underwater robot," *Bioinspiration Biomimetics*, vol. 9, no. 3, Mar. 2014, Art. no. 036002, doi: 10.1088/1748-3182/9/3/036002.
[22] B. Chen and H. Jiang, "Body stiffness variation of a tensegrity robotic fish using antagonistic stiffness in a kinematically singular configuration," *IEEE Trans. Robot.*, vol. 37, no. 5, pp. 1712–1727, Oct. 2021.
[23] X. Dong, Z. Haining, P. Xiang, Z. Ziqing, and L. Jingmeng, "A stiffness adjustment mechanism based on negative work for high-efficient propulsion of robotic fish," *J. Bionic Eng.*, vol. 15, no. 2, 2018, Art. no. 270. [Online]. Available: http://jbe.jlu.edu.cn/EN/abstract/article_613.shtml
[24] J. Yu, Z. Su, Z. Wu, and M. Tan, "Development of a fast-swimming dolphin robot capable of leaping," *IEEE/ASME Trans. Mechatron.*, vol. 21, no. 5, pp. 2307–2316, Oct. 2016.
[25] Q. Zou, C. Zhou, B. Lu, X. Liao, and Z. Zhang, "Tail-stiffness optimization for a flexible robotic fish," *Bioinspiration Biomimetics*, vol. 17, no. 6, Sep. 2022, Art. no. 066003, doi: 10.1088/1748-3190/ac84b6.
[26] D. Chen, Z. Wu, P. Zhang, M. Tan, and J. Yu, "Performance improvement of a high-speed swimming robot for fish-like leaping," *IEEE Robot. Automat. Lett.*, vol. 7, no. 2, pp. 1936–1943, Apr. 2022.
[27] D. Chen, Z. Wu, Y. Meng, M. Tan, and J. Yu, "Development of a high-speed swimming robot with the capability of fish-like leaping," *IEEE/ASME Trans. Mechatron.*, vol. 27, no. 5, pp. 3579–3589, Oct. 2022.
[28] M. C. Leftwich, E. D. Tytell, A. H. Cohen, and A. J. Smits, "Wake structures behind a swimming robotic lamprey with a passively flexible tail," *J. Exp. Biol.*, vol. 215, no. 3, pp. 416–425, 2012, doi: 10.1242/jeb.061440.
[29] J. Long et al., "Testing biomimetic structures in bioinspired robots: How vertebrae control the stiffness of the body and the behavior of fish-like swimmers," *Integrative Comp. Biol.*, vol. 51, no. 1, pp. 158–175, 2011, doi: 10.1093/icb/icr020.
[30] B. Chen and H. Jiang, "Swimming performance of a tensegrity robotic fish," *Soft Robot.*, vol. 6, no. 4, pp. 520–531, 2019, doi: 10.1089/soro.2018.0079.
[31] B. Lu, C. Zhou, J. Wang, Y. Fu, L. Cheng, and M. Tan, "Development and stiffness optimization for a flexible-tail robotic fish," *IEEE Robot. Automat. Lett.*, vol. 7, no. 2, pp. 834–841, Apr. 2022.
[32] H. F. Schulte, "The characteristics of the McKibben artificial muscle," *Appl. External Power Prosthetics Orthotics*, pp. 94–115, 1961. [Online]. Available: https://cir.nii.ac.jp/crid/1573387450709810432
[33] R. M. Alexander, "The orientation of muscle fibres in the myomeres of fishes," *J. Mar. Biol. Assoc. United Kingdom*, vol. 49, no. 2, pp. 263–290, 1969.
[34] D. K. Wainwright and G. V. Lauder, "Tunas as a high-performance fish platform for inspiring the next generation of autonomous underwater vehicles," *Bioinspiration Biomimetics*, vol. 15, no. 3, Mar. 2020, Art. no. 035007, doi: 10.1088/1748-3190/ab75f7.
[35] J. Zhu, C. White, D. K. Wainwright, V. D. Santo, G. V. Lauder, and H. Bart-Smith, "Tuna robotics: A high-frequency experimental platform exploring the performance space of swimming fishes," *Sci. Robot.*, vol. 4, no. 34, Art. no. eaax4615, 2019, doi: 10.1126/scirobotics.aax4615.
[36] W. Wang and S.-H. Ahn, "Shape memory alloy-based soft gripper with variable stiffness for compliant and effective grasping," *Soft Robot.*, vol. 4, no. 4, pp. 379–389, 2017, doi: 10.1089/soro.2016.0081.
[37] S. Liu, Y. Wang, Z. Li, M. Jin, L. Ren, and C. Liu, "A fluid-driven soft robotic fish inspired by fish muscle architecture," *Bioinspiration Biomimetics*, vol. 17, no. 2, Feb. 2022, Art. no. 026009, doi: 10.1088/1748-3190/ac4afb.
[38] C. Eloy, "Optimal strouhal number for swimming animals," *J. Fluids Struct.*, vol. 30, pp. 205–218, 2012. [Online]. Available: https://www.sciencedirect.com/science/article/pii/S0889974612000503
[39] G. K. Taylor, R. L. Nudds, and A. L. Thomas, "Flying and swimming animals cruise at a strouhal number tuned for high power efficiency," *Nature*, vol. 425, no. 6959, pp. 707–711, 2003.
[40] M. S. Triantafyllou, G. S. Triantafyllou, and R. Gopalkrishnan, "Wake mechanics for thrust generation in oscillating foils," *Phys. Fluids A: Fluid Dyn.*, vol. 3, no. 12, pp. 2835–2837, 1991, doi: 10.1063/1.858173.
[41] M. S. Triantafyllou, G. S. Triantafyllou, and D. K. P. Yue, "Hydrodynamics of fishlike swimming," *Annu. Rev. Fluid Mechanics*, vol. 32, no. 1, pp. 33–53, 2000, doi: 10.1146/annurev.fluid.32.1.33.
[42] D. B. Quinn, G. V. Lauder, and A. J. Smits, "Maximizing the efficiency of a flexible propulsor using experimental optimization," *J. Fluid Mechanics*, vol. 767, pp. 430–448, 2015.
[43] Z. Ren, X. Yang, T. Wang, and L. Wen, "Hydrodynamics of a robotic fish tail: Effects of the caudal peduncle, fin ray motions and the flow speed," *Bioinspiration Biomimetics*, vol. 11, no. 1, Feb. 2016, Art. no. 016008, doi: 10.1088/1748-3190/11/1/016008.
[44] J. Wang, D. K. Wainwright, R. E. Lindengren, G. V. Lauder, and H. Dong, "Tuna locomotion: A computational hydrodynamic analysis of finlet function," *J. Roy. Soc. Interface*, vol. 17, no. 165, 2020, Art. no. 20190590, doi: 10.1098/rsif.2019.0590.
[45] J. Wang, G. Lauder, and H. Dong, "Effect of tunable stiffness on the hydrodynamic performance of a tuna tail informed flexible propulsor," in *Proc. AIAA SCITECH Forum*, 2022, pp. 1–10.
[46] B. C. Jayne and G. V. Lauder, "Are muscle fibers within fish myotomes activated synchronously? Patterns of recruitment within deep myomeric musculature during swimming in largemouth bass," *J. Exp. Biol.*, vol. 198, no. 3, pp. 805–815, 1995, doi: 10.1242/jeb.198.3.805.
[47] E. D. Tytell and G. V. Lauder, "The C-start escape response of polypterus senegalus: Bilateral muscle activity and variation during stage 1 and 2," *J. Exp. Biol.*, vol. 205, no. 17, pp. 2591–2603, 2002, doi: 10.1242/jeb.205.17.2591.